ES10 - A NenuFAR study of Radio Recombination Lines towards the Cas A SNR

Lucie Cros, LPENS, ENS (M1 internship : 4 months)
PIs : Antoine Gusdorf, LPENS, ENS & Philippe Salomé, LERMA, OP
Jonathan Freundlich, OBAS
Pedro Salas, NRAO

Outline

- Scientific objectives
- Reduction pipeline
- Detections
- Results
- Perspectives

Scientific objectives

The interstellar medium of galaxies

- The medium between the stars of a galaxy, where the stars are born

- Multiphase:
  - gas & grains (1% of mass)
  - diverse ionization states/fractions
  - diverse densities (~10-3 to 106 cm-3)
  - diverse temperatures (~10 to 106 K)

- Multi-scales, with coupled scales:
  - from giant molecular clouds (~10 pc)
  - to proto-planetary disks (~10 AU)

- irradiated by diverse fields:
  - from radio to gamma photons
  - magnetic fields

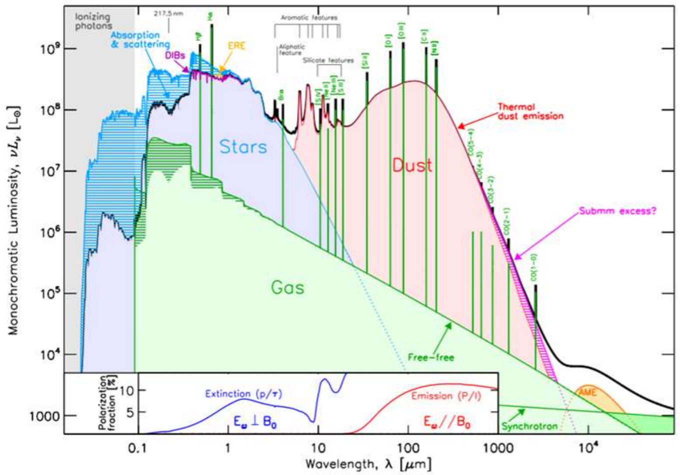

The interstellar medium cycle

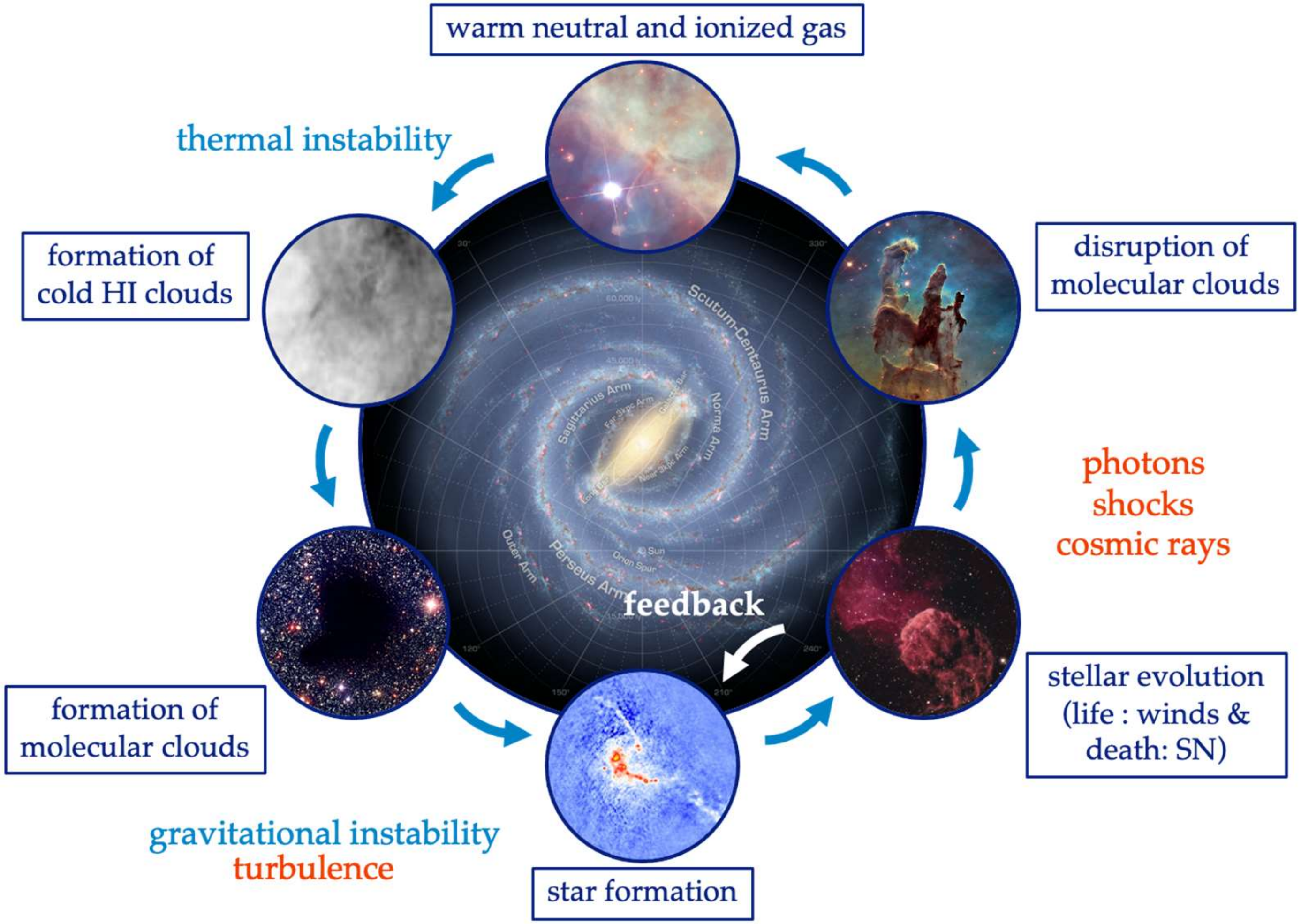

The interstellar medium cycle

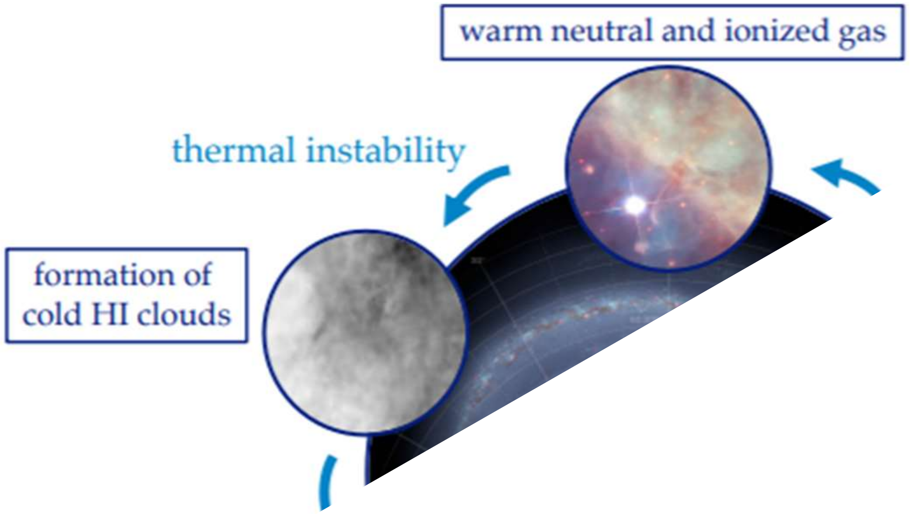

- Scientific question of ES10 :
  - How does the interstellar medium transform its gas in stars ?
  - Specifically targeting the neutral/ionized stage of the process

The interstellar medium cycle

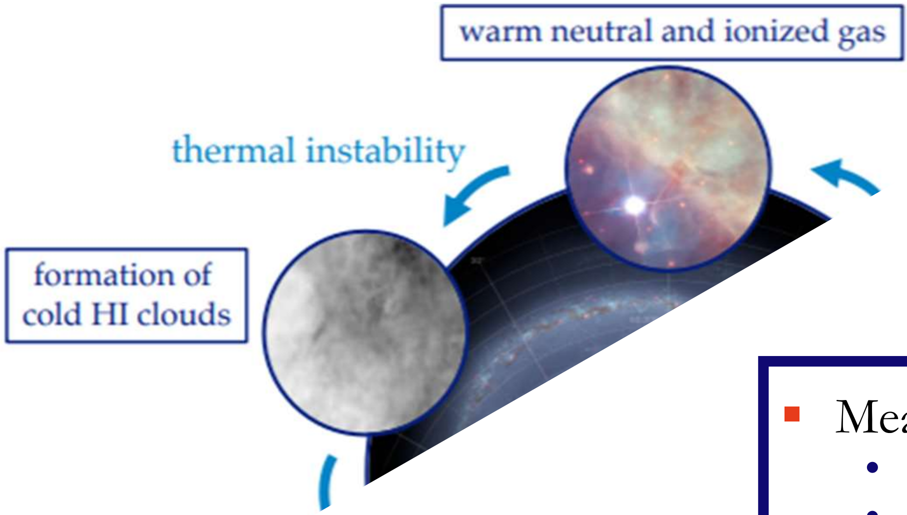

- Means to achieve this goal :
  - Observation of RRLs (H, He, C)
  - Interpretation to constrain (n_e, T_e)
  - Towards Faraday tomography experiments

- Scientific question of ES10 :
  - How does the interstellar medium transform its gas in stars ?
  - Specifically targeting the neutral/ionized stage of the process

Recombination line : Atomic structure of Hydrogen

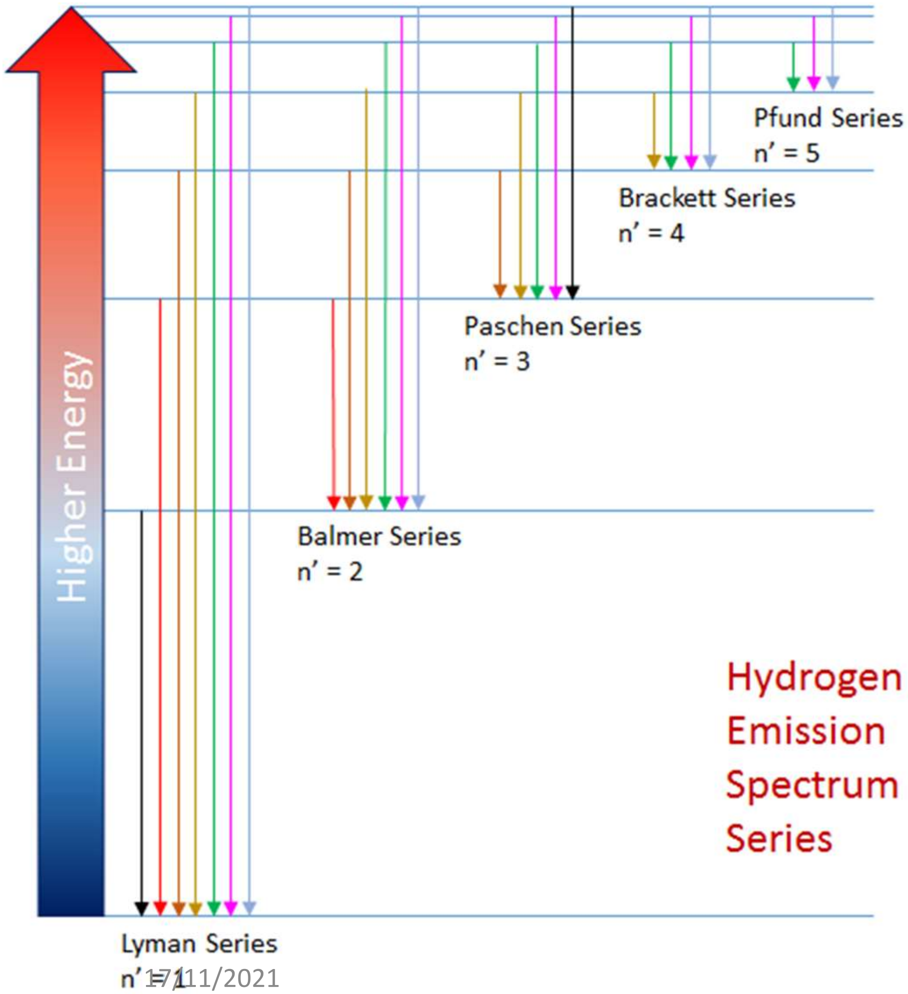

- Rydberg equation :

$$E = -\frac{\mu e^4}{2\hbar^2}\frac{1}{n^2} = -hcR_H\frac{1}{n^2}$$

- With R_H = 109,677.585 cm^{-1} : Rydberg constant for H

- E(ionization) = 13.6 V for H

➢ Carbon has a **lower ionization potential** (11.2eV) than hydrogen and can be ionized by radiation fields in regions where hydrogen is largely neutral.

Radio Recombination Lines (RRLs)

➢ WHAT ?

- **Classical RRLs associated with H II regions (Palmer 1967)**
    - Recombination lines from hydrogen, helium and carbon (e.g. Konovalenko & Stepkin 2005). Predominantly observed at frequencies >1 GHz as they trace the warm ($T_e \sim 10^4$ K), high-density ($n_e > 100$ cm^{-3}) gas.
- **Diffuse RRLs associated with the low-density, cold interstellar medium (e.g. Konovalenko & Sodin 1981; Payne et al. 1989)**
    - Only RRLs from carbon (CRRL) typically observed as the ionization levels are too low to produce hydrogen and helium lines. Diffuse CRRLs are best observed at radio frequencies below 1 GHz because they arise from stimulated emission and absorption.

➢ WHY ?

- **Emitting in the radio domain so unbiased by dust obscuration**
- **Measure the temperature, density and ionization of the cold neutral medium**

➢ HOW ?

- **Studying the optical depth and width of the lines as a function of their quantum number (e.g. Dupree 1971; Shaver 1975, 1976a; Salem & Brocklehurst 1979; Walmsley & Watson 1982)**

Line/continuum ratio

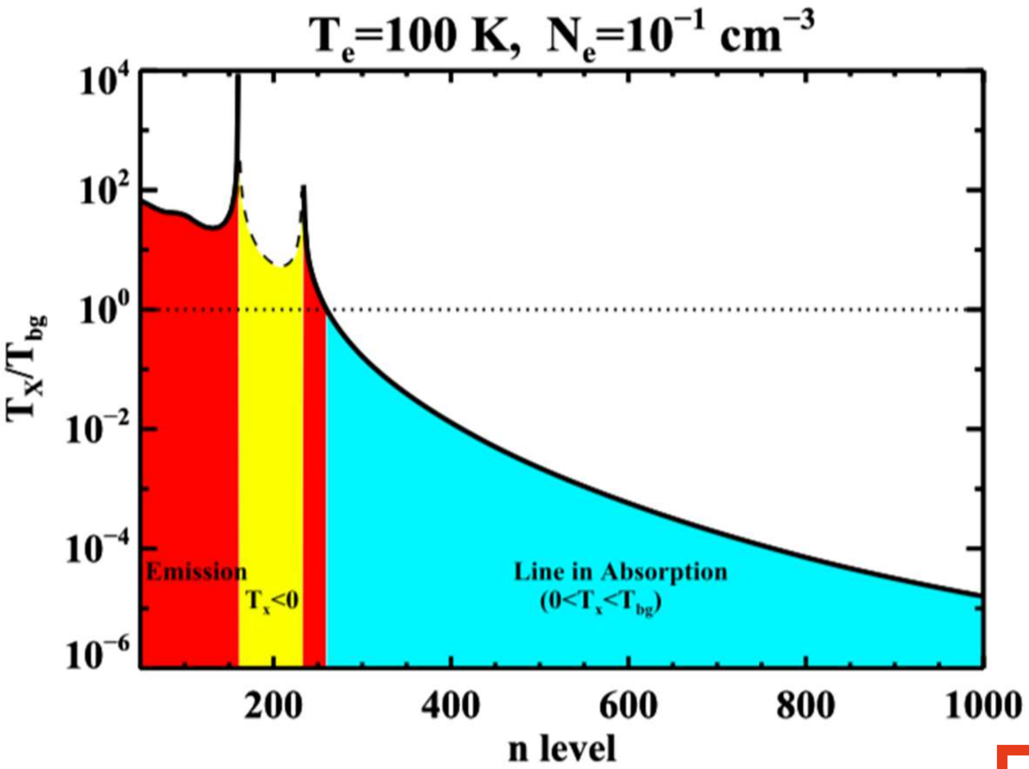

Integrated optical depth = $f(T_e, n_e)$

$$\int \frac{I_\nu^{line}}{I_\nu^{cont}}\, d\nu = -0.2\, b_n \beta_{nn'} \left(\frac{T_e}{100\ \mathrm{K}}\right)^{-2.5} \left(\frac{N_e}{0.1\ \mathrm{cm}^{-3}}\right)^{2} \left(\frac{L}{\mathrm{pc}}\right) \mathrm{Hz}$$

Linewidth : Voigt Profile

- Gaussian line profile :
  - Doppler (thermal) broadening :

$$(\Delta\nu_D)^2 = \left(\frac{\nu_0}{c}\right)^2 \left(\frac{2kT_e}{m_c}\right)$$

  - Turbulence broadening :

$$(\Delta\nu_T)^2 = \left(\frac{\nu_0}{c}\right)^2 \langle v_{rms}\rangle^2$$

  - Gaussian broadening :

$$\Delta\nu_G = \frac{\nu_0}{c}\sqrt{\frac{2kT_e}{m_c} + \langle v_{rms}\rangle^2 + \delta v^2}$$

- Lorentz line profile :
  - Collision broadening :

$$\Delta\nu_{col} = \frac{1}{\pi}\sum_{n\neq n\prime} N_e C_{n\prime n}$$

  - Radiation broadening :

$$\Delta\nu_{rad} = 6.096 \times 10^{-17} T_0 n^{5.8}\ (s^{-1})$$

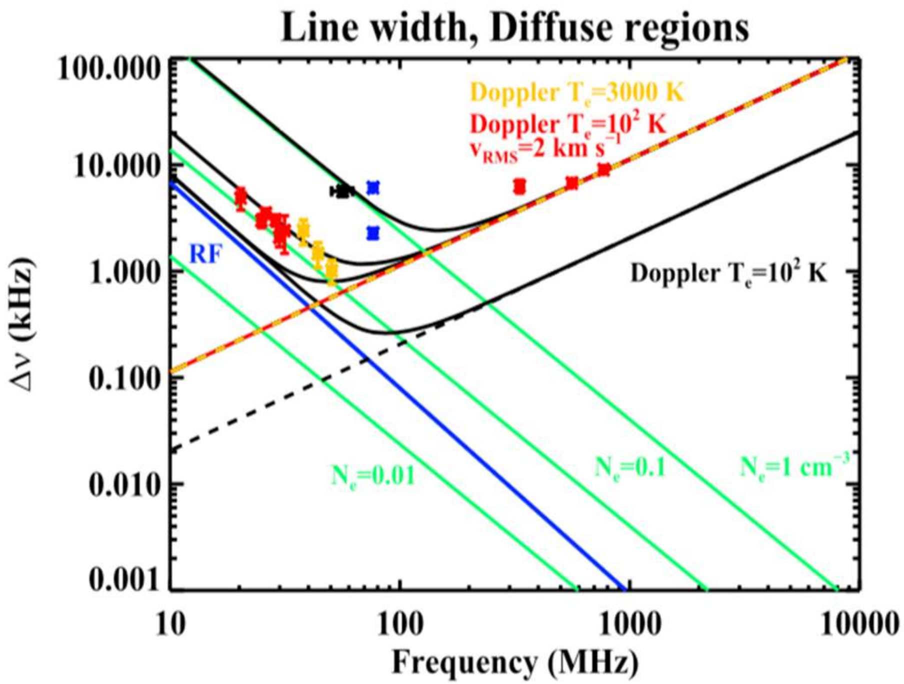

Figure 3. A comparison between broadening produced by the Galactic radiation field (blue line), collisional broadening at $N_e = 1,\ 0.1,$ and 0.01 cm^{-3} (green lines), and thermal (Doppler) broadening at 100 K (black dashed line). The red and yellow curves correspond to a turbulent Doppler parameter $\langle v_{\rm rms}\rangle^2 = 2$ km s^{-1} and $T_e = 300$ K, respectively. We include data for Cas A (Payne et al. 1994; Kantharia et al. 1998) as red points, Cyg A (Oonk et al. 2014) as yellow points, regions for the inner galaxy (Erickson et al. 1995) as blue points, and data for M82 (Morabito et al. 2014) as a black point.

Cassiopeia A : general presentation

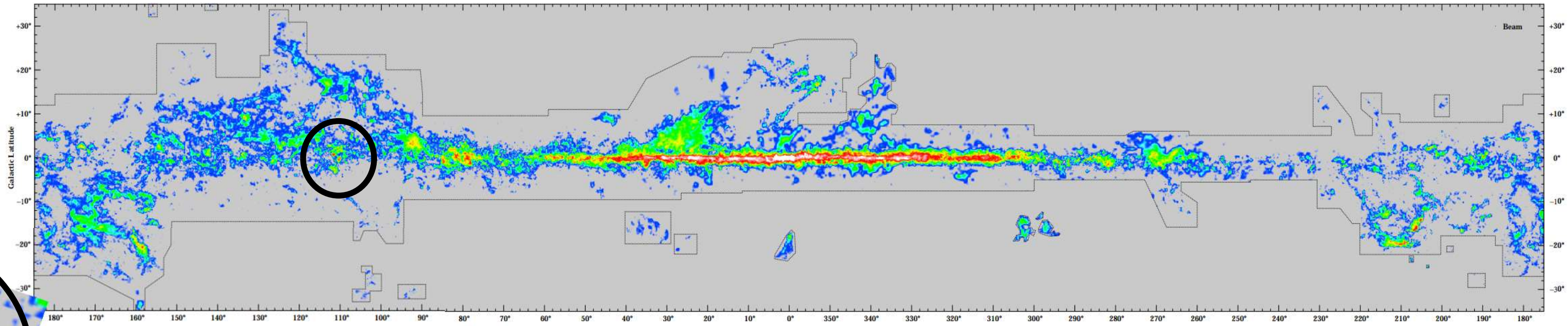

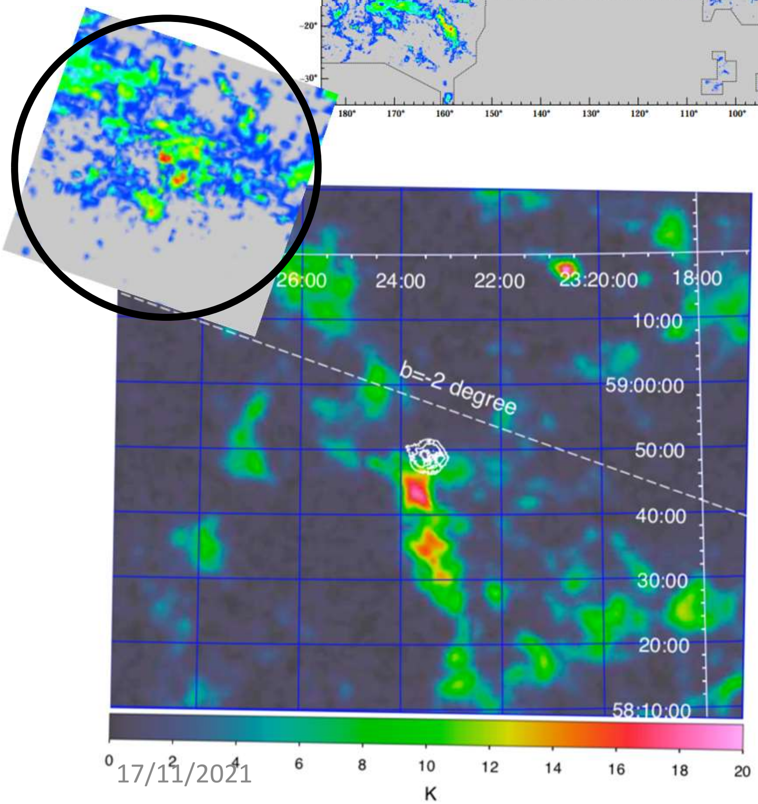

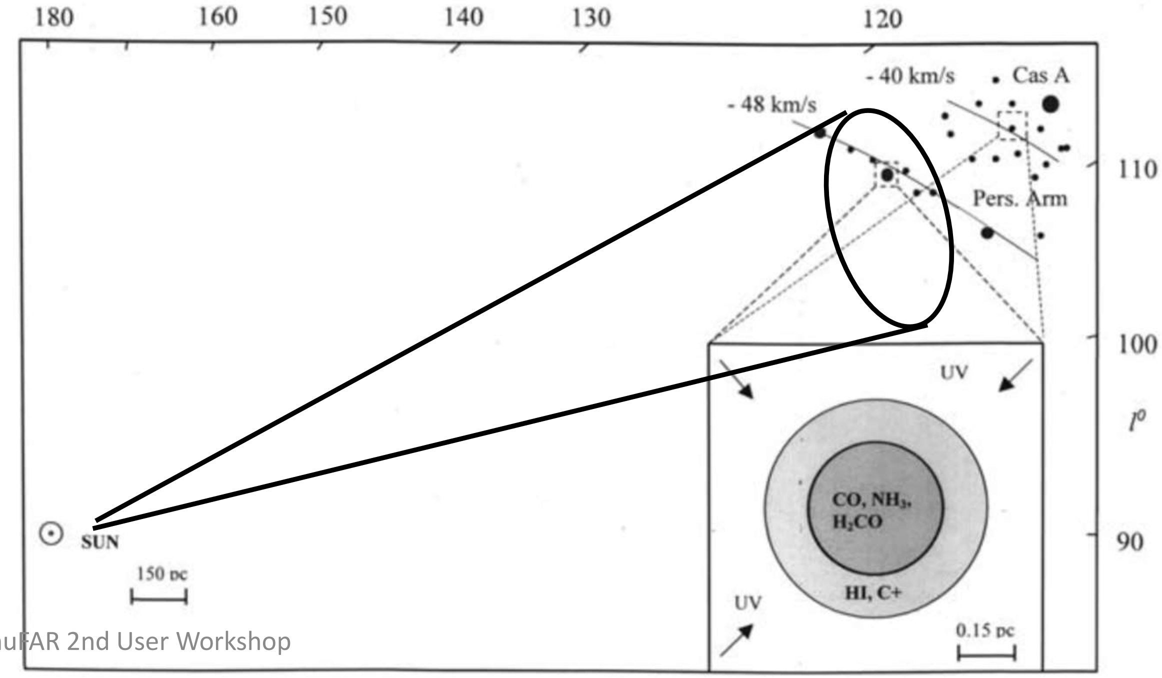

Cassiopeia A : cartography

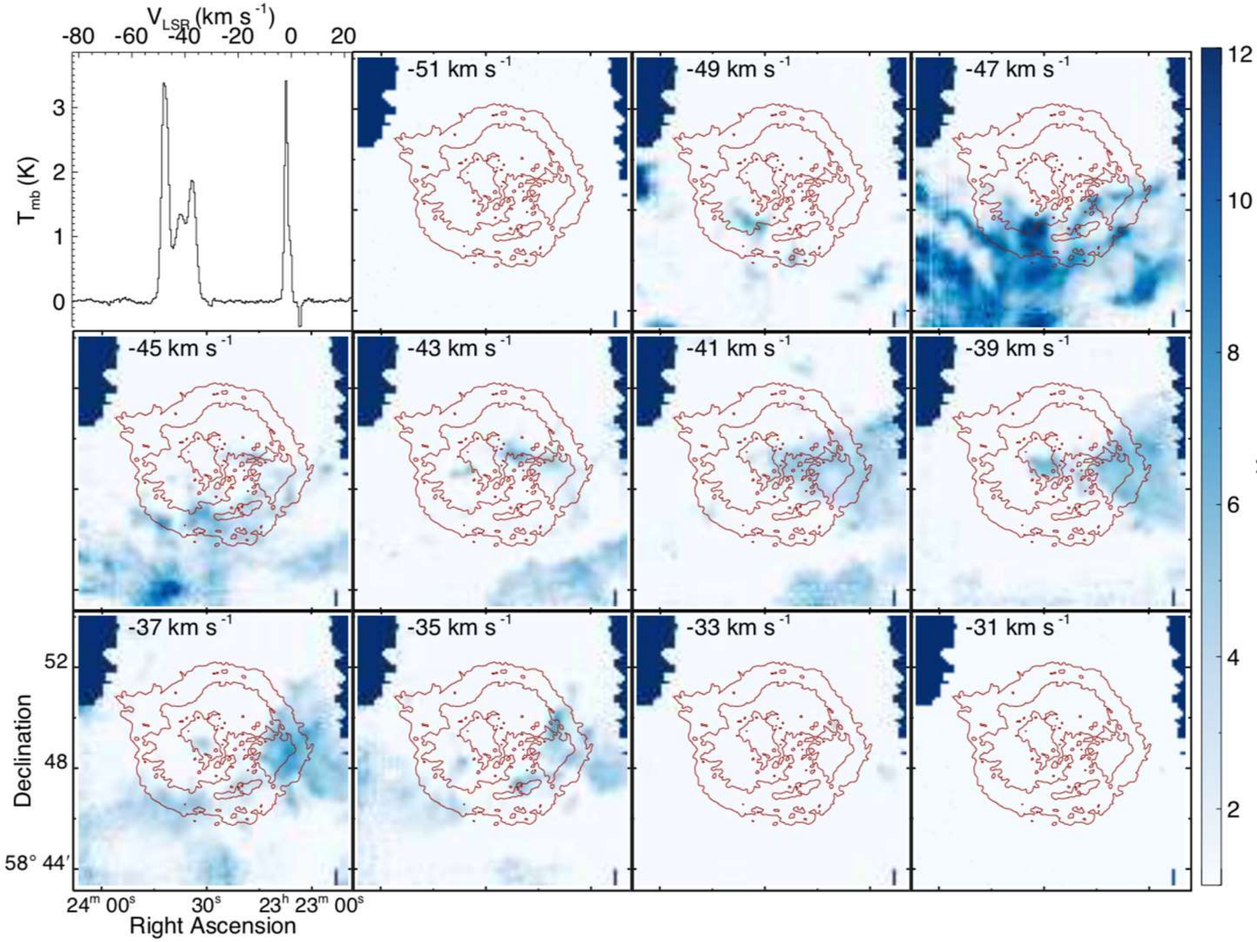

Cassiopeia A with LOFAR

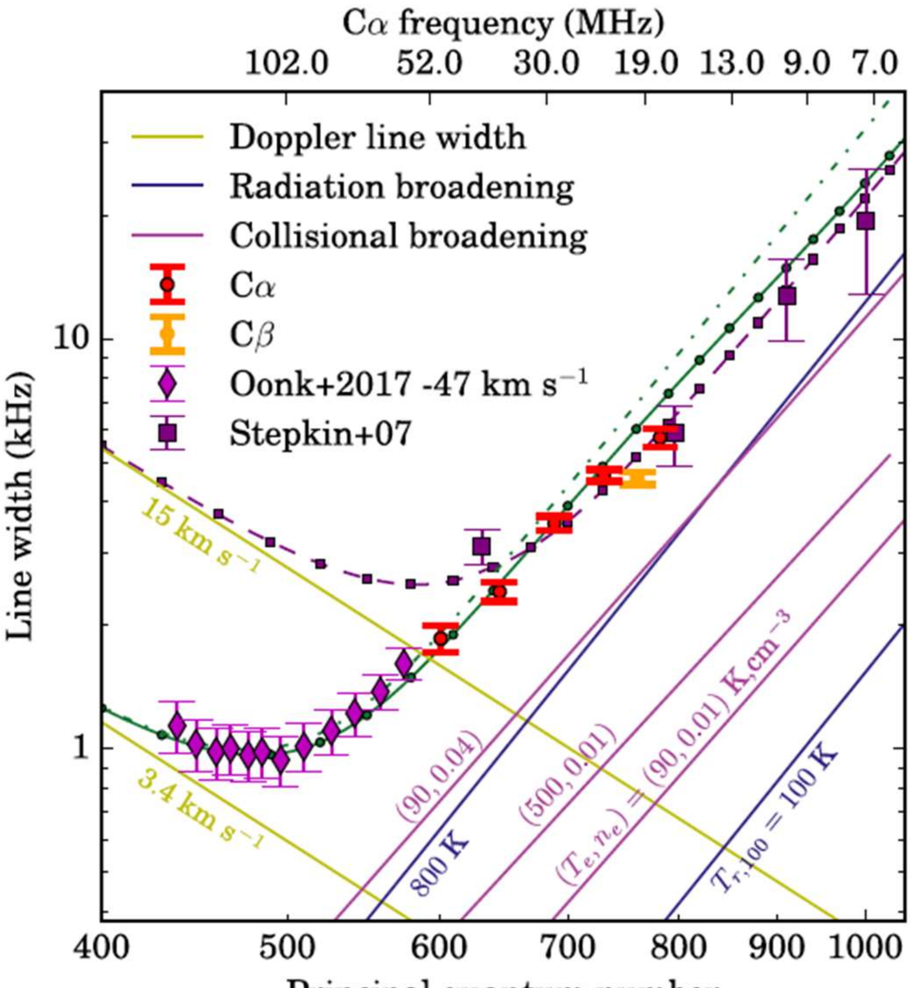

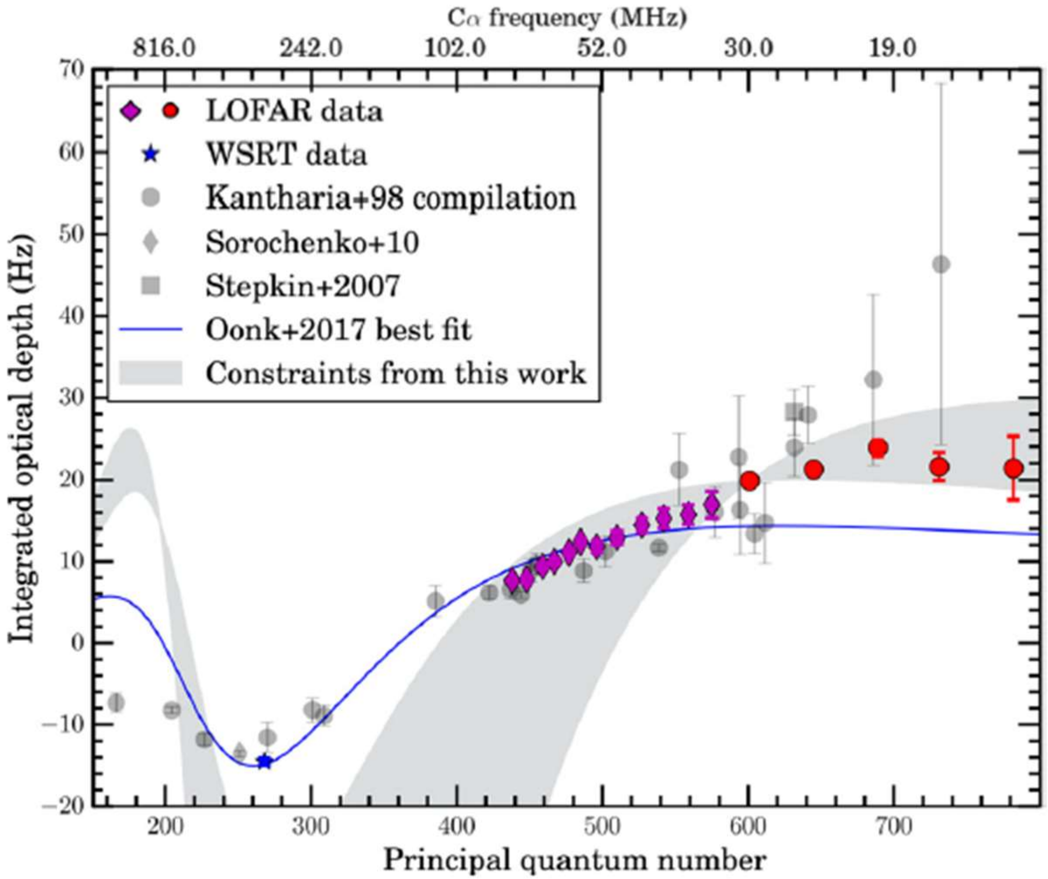

Cassiopeia A with NenuFAR : available data

Towards Cassiopeia A, the CRRLs are associated with low-density (n_e ~0.1cm^{-3}), cold (T_e ~70K) intervening clouds in the Perseus and Orion spiral arms (e.g. PAE89; Kantharia, Anantharamaiah & Payne 1998)

Parameter	Value	
Source	Cas A	
Field centre RA (J2000)	23 :23 :24.0	
Field centre Dec. (J2000)	58 :48 :54	
Observing date	2019 September 15	18h-20h
Observing date	2019 September 15	20h-22h
Observing date	2019 September 15	22h-00h
Observing date	2019 October 4	18h30-20h30
Observing date	2019 October 4	20h30-22h30
Observing date	2019 October 4	22h30-00h30
Observing date	2019 October 5	00h30-02h30
Observing date	2019 October 5	02h30-03h58
Observing date	2019 October 5	16h30-18h30
Observing date	2019 October 5	18h30-20h30
Observing date	2019 October 5	20h30-22h30
Observing date	2019 October 5	22h30-00h30
Observing date	2019 October 6	00h30-02h30
Observing date	2021 September 19	23h-01h
Observing date	2021 September 20	01h-03h

Cassiopeia A with NenuFAR : rms estimate

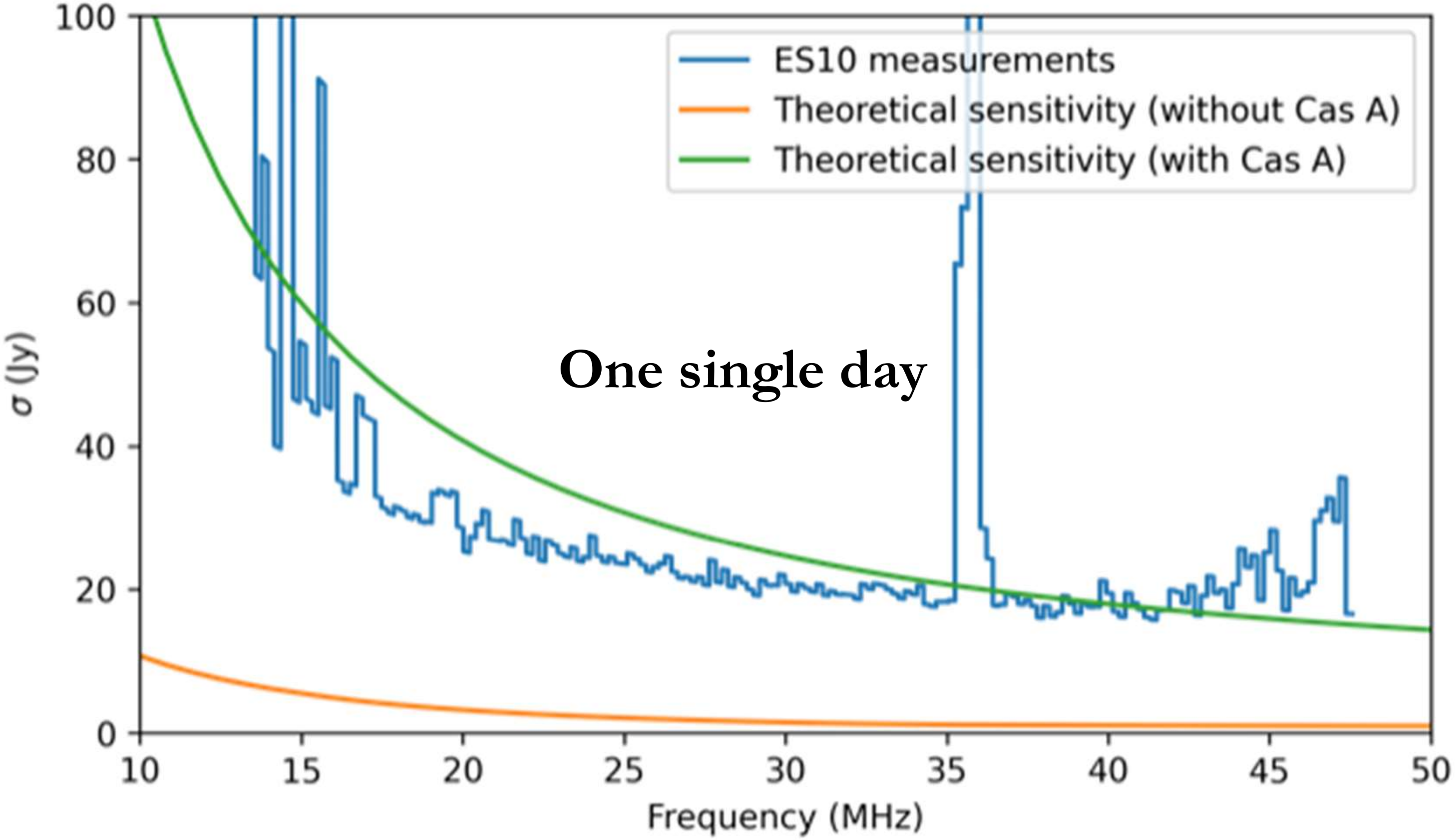

Measured noise consistent with estimated noise from Nenupy by Alan Loh

- Decoherence = 1
- Elevation = 60deg
- 56 Mini-Arrays

Reduction

Reduction principles

- Integration of the data : from 2D to 1D data
- Locating expected lines : protecting the potential detections
- Flattening : from relative intensity to optical depth
- Cleaning : RFI mitigation

Integration

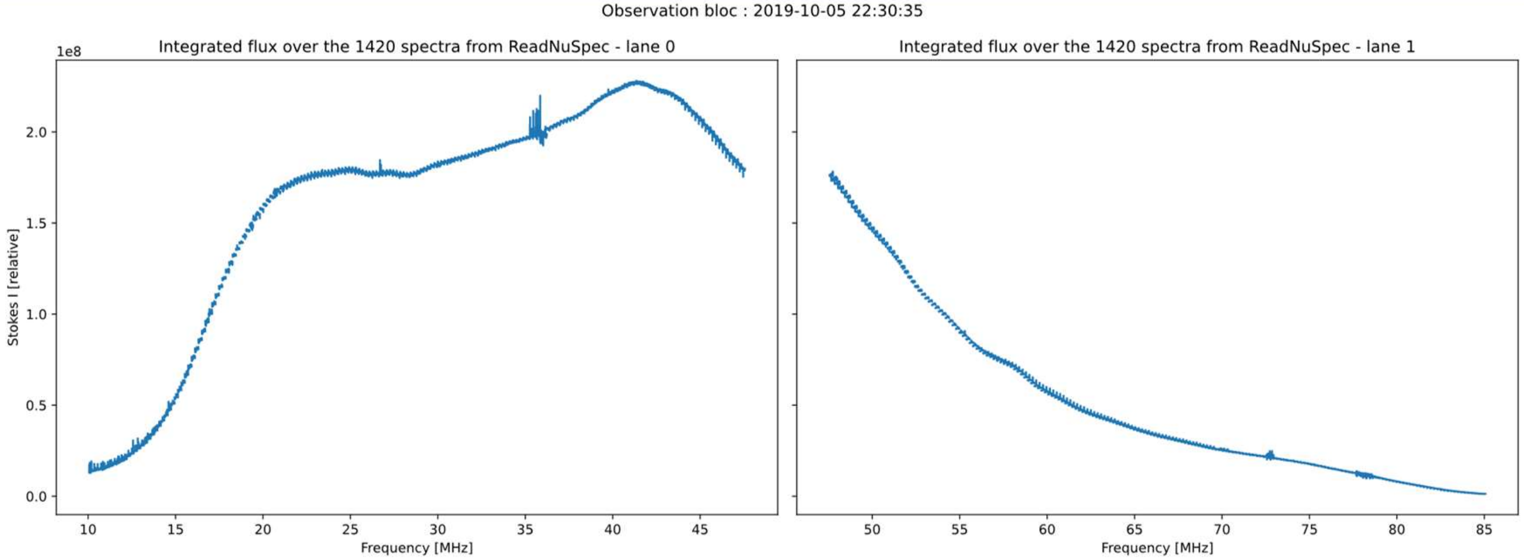

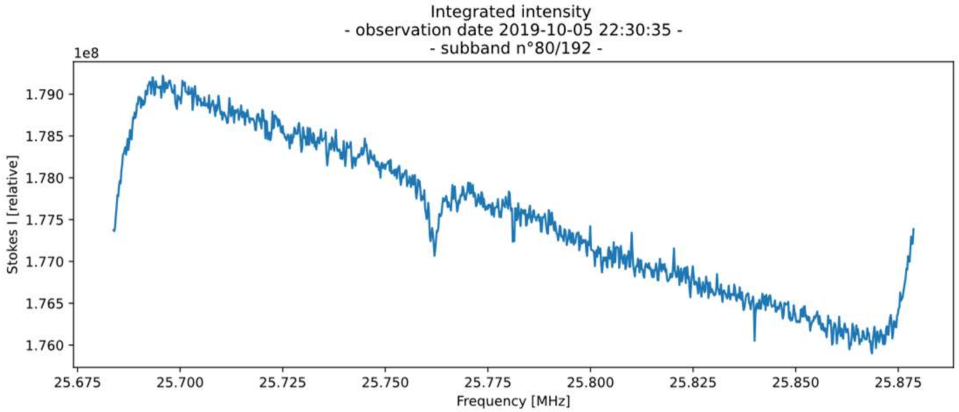

Protecting the expected lines

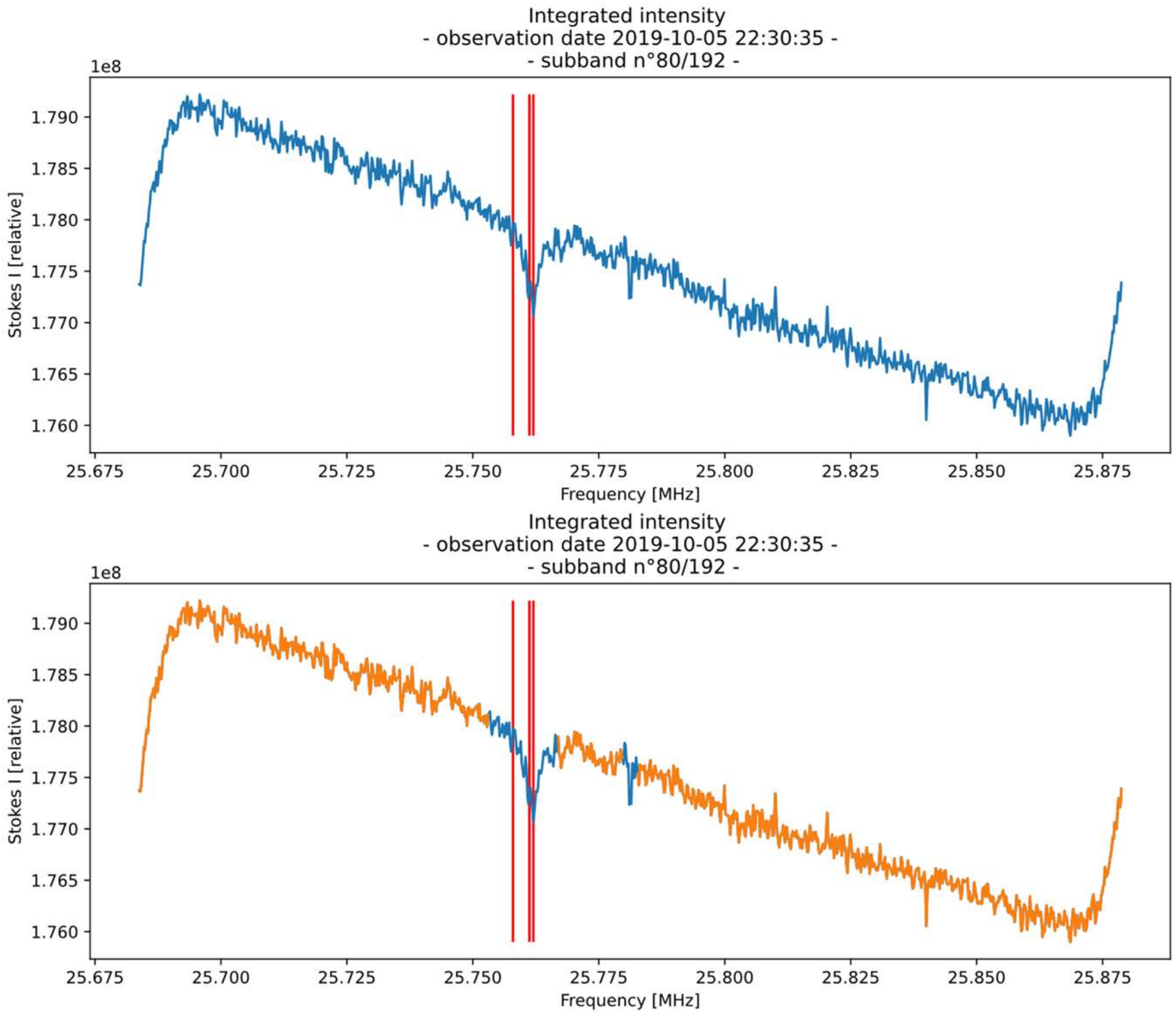

Velocity components along the line of sight :

Location	**Galactic reference frame**	**LSR**
Perseus spiral arm	-47 km/s	-61.35 km/s
Perseus spiral arm	-38 km/s	-52.35 km/s
Orion arm	0 km/s	-14.35 km/s

Flattening

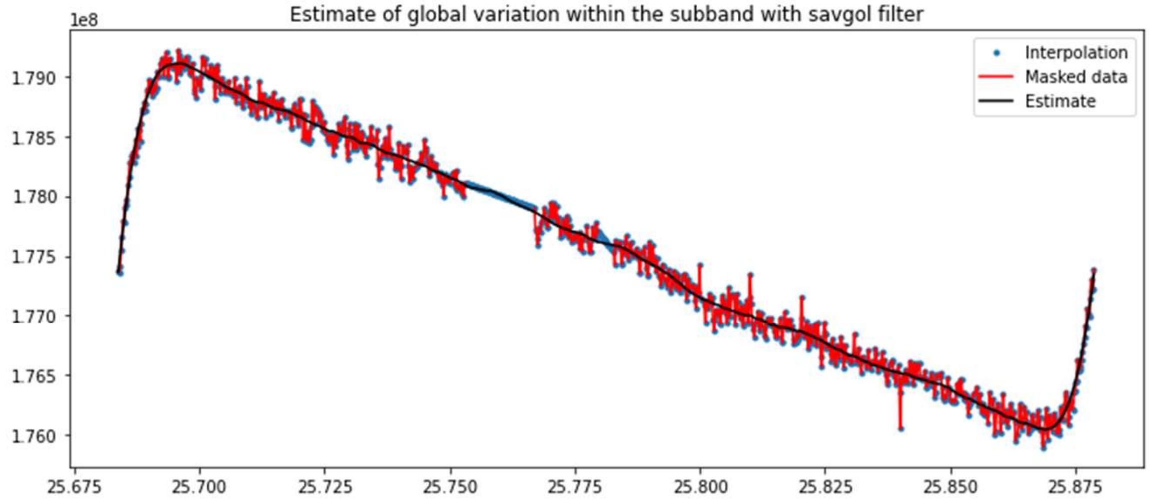

Estimate of global variation within the subband with savgol filter
1e8
1.790
1.785
1.780
1.775
1.770
1.765
1.760
25.675
25.700
25.725
25.750
25.775
25.800
25.825
25.850
25.875
Interpolation
Masked data
Estimate

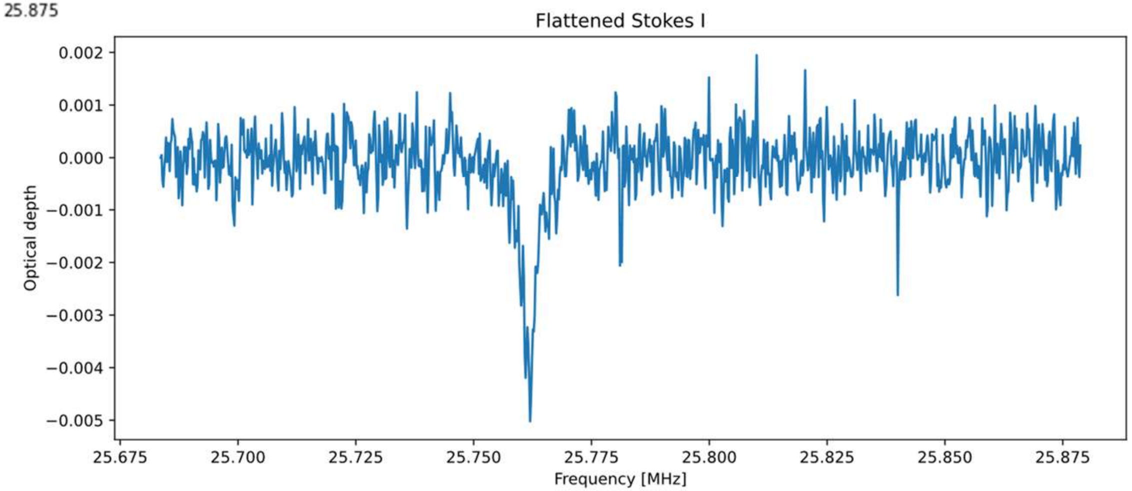

Flattened Stokes I
Optical depth
0.002
0.001
0.000
−0.001
−0.002
−0.003
−0.004
−0.005
25.675
25.700
25.725
25.750
25.775
25.800
25.825
25.850
25.875
Frequency [MHz]

Cleaning

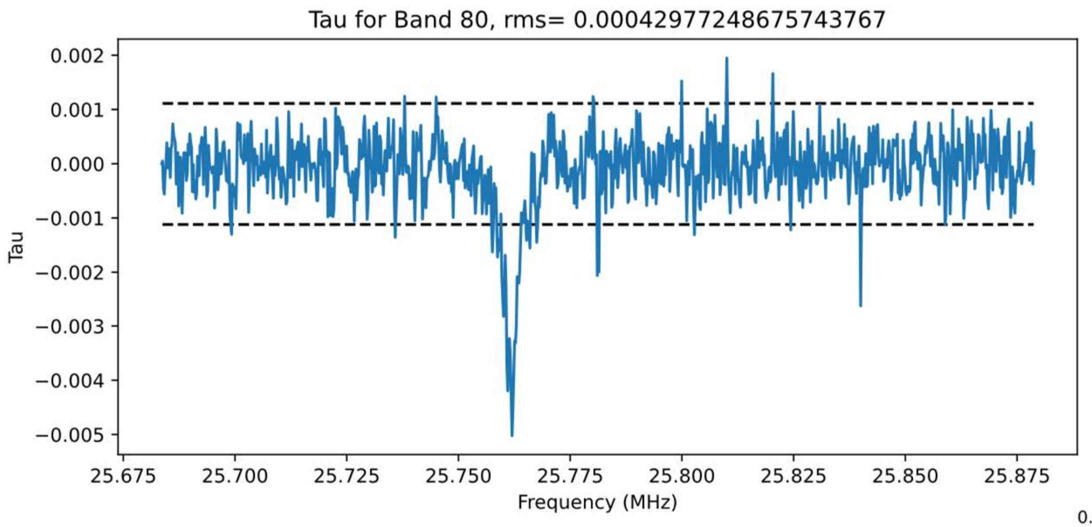

Tau for Band 80, rms= 0.00042977248675743767
0.002
0.001
0.000
−0.001
−0.002
−0.003
−0.004
−0.005
Tau
25.675
25.700
25.725
25.750
25.775
25.800
25.825
25.850
25.875
Frequency (MHz)

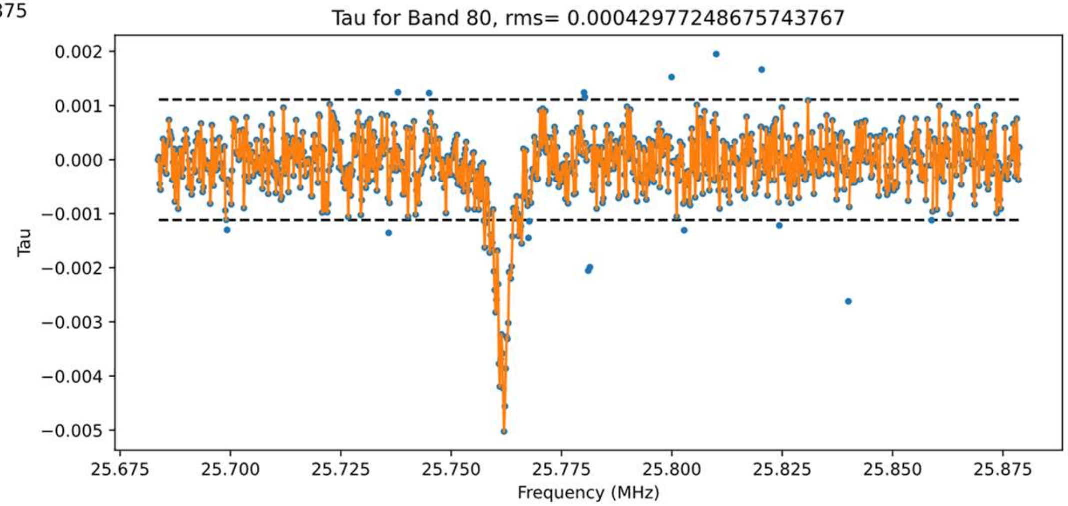

Tau for Band 80, rms= 0.00042977248675743767
0.002
0.001
0.000
−0.001
−0.002
−0.003
−0.004
−0.005
Tau
25.675
25.700
25.725
25.750
25.775
25.800
25.825
25.850
25.875
Frequency (MHz)

RRL detections

Detection principles

- Locating expected lines (with LSR correction)
- Slicing : selection of a window around the expected line
- 2nd cleaning
- Fitting to a voigt model
- Available extra processing steps :
  - Averaging the subbands on all the observation blocks
  - Stacking the lines along the frequency axis

Locating and selecting expected lines

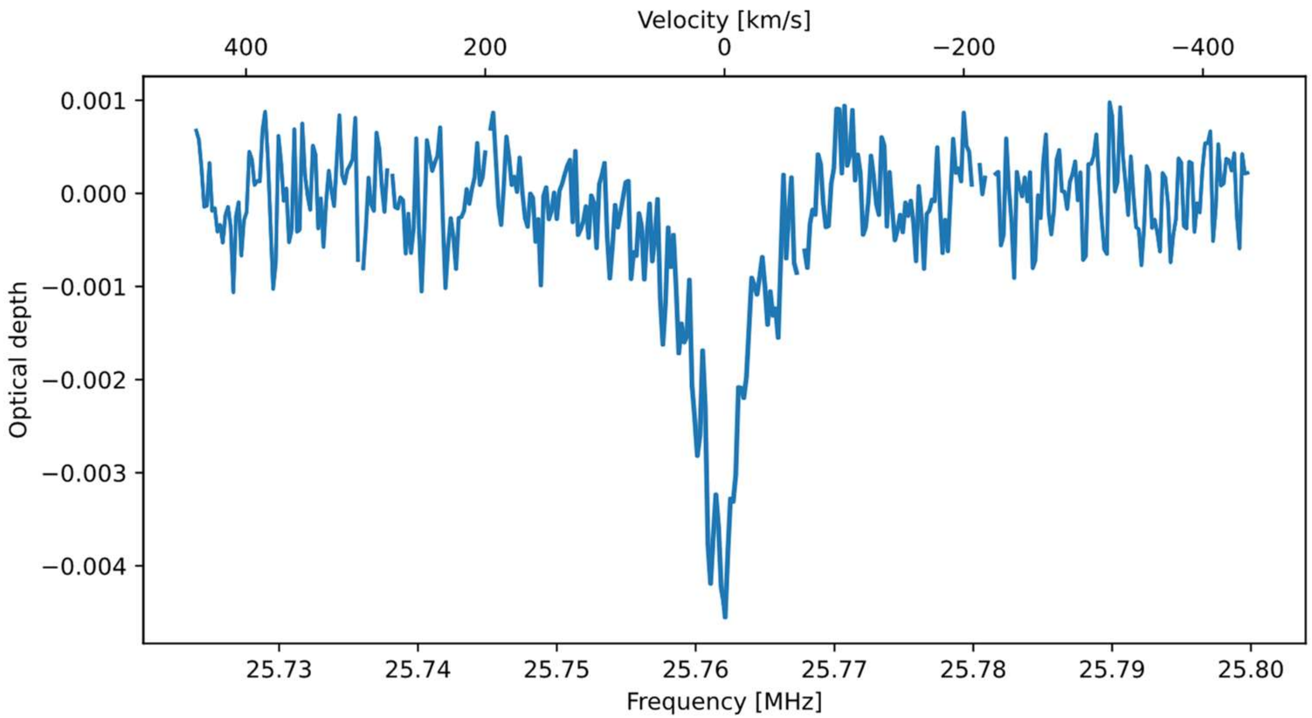

2nd cleaning phase

Exemple of the 40-th subband

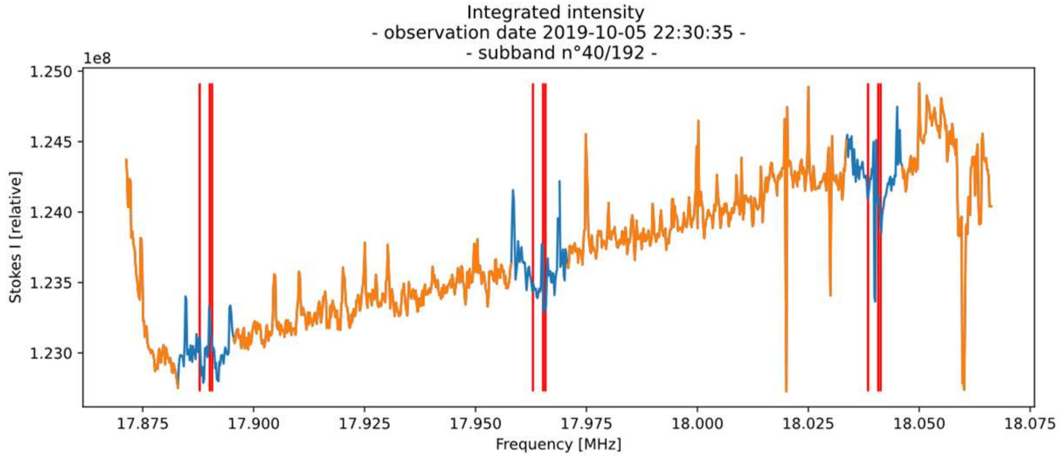

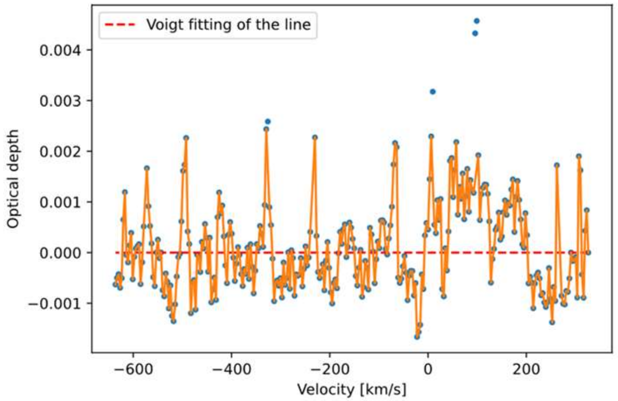

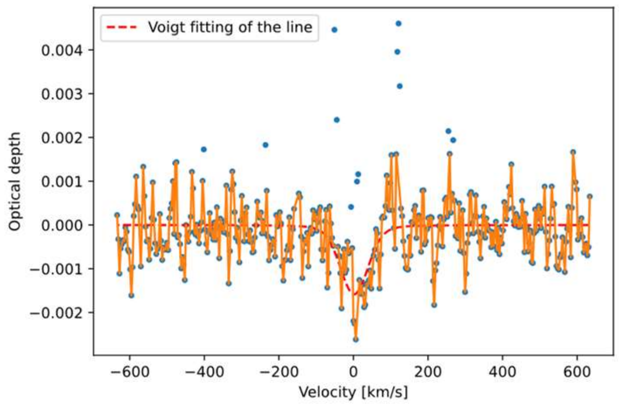

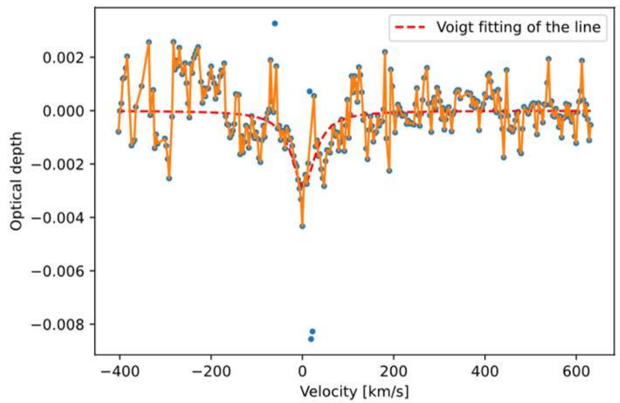

Fitting expected lines

2019-10-05 / 00:31:36

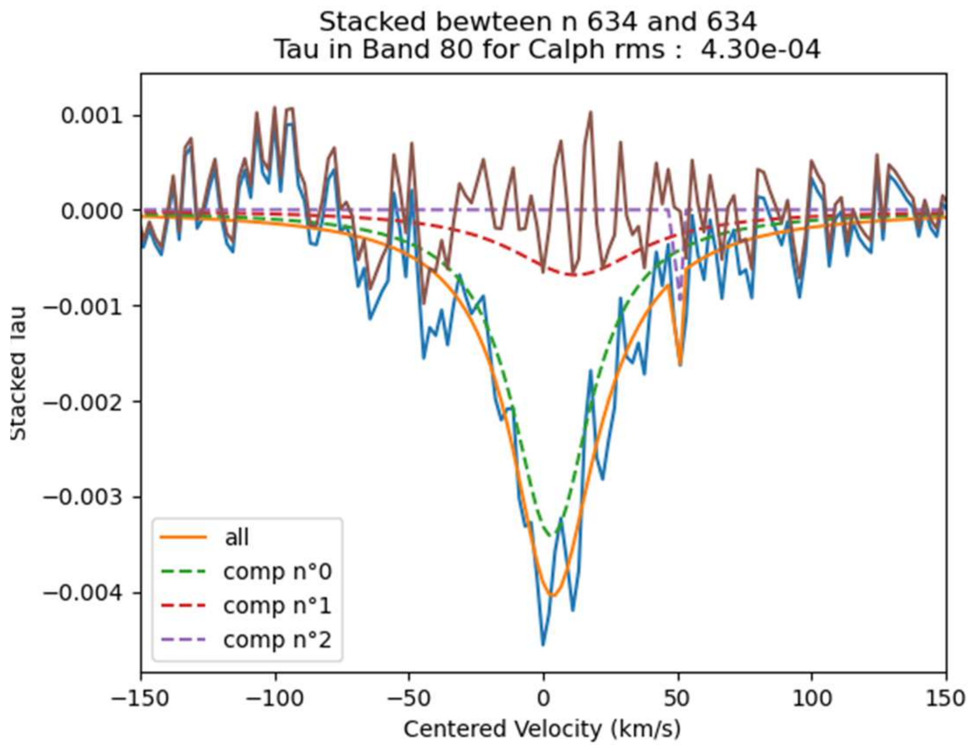

2019-10-05 / 22:30:35

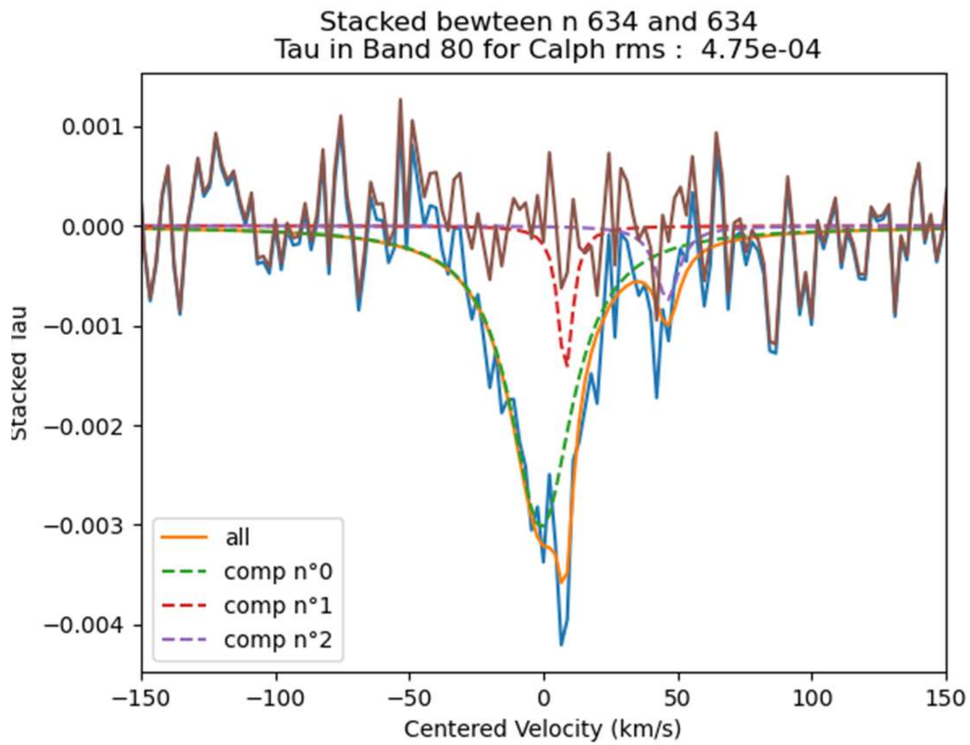

Average

- Average over 9*2 hours on source observation
- Weighted with 1/rms² of residuals of each detection

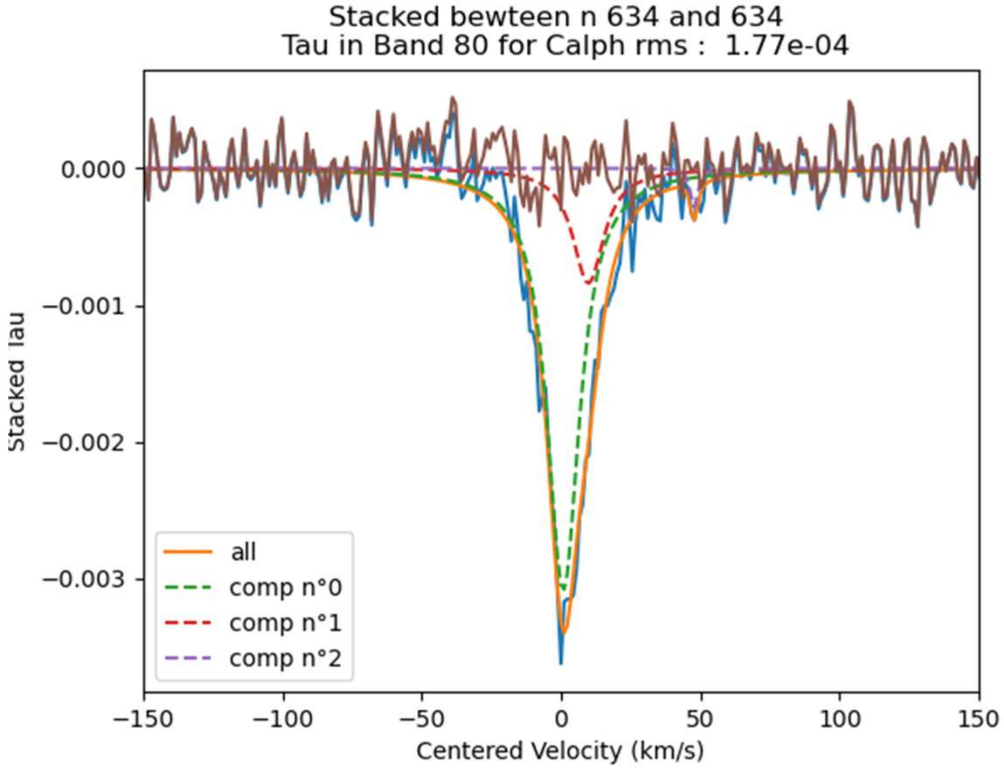

Stacking along frequency axis

From subband 80 to subband 100 : 29 lines (on averaged data)

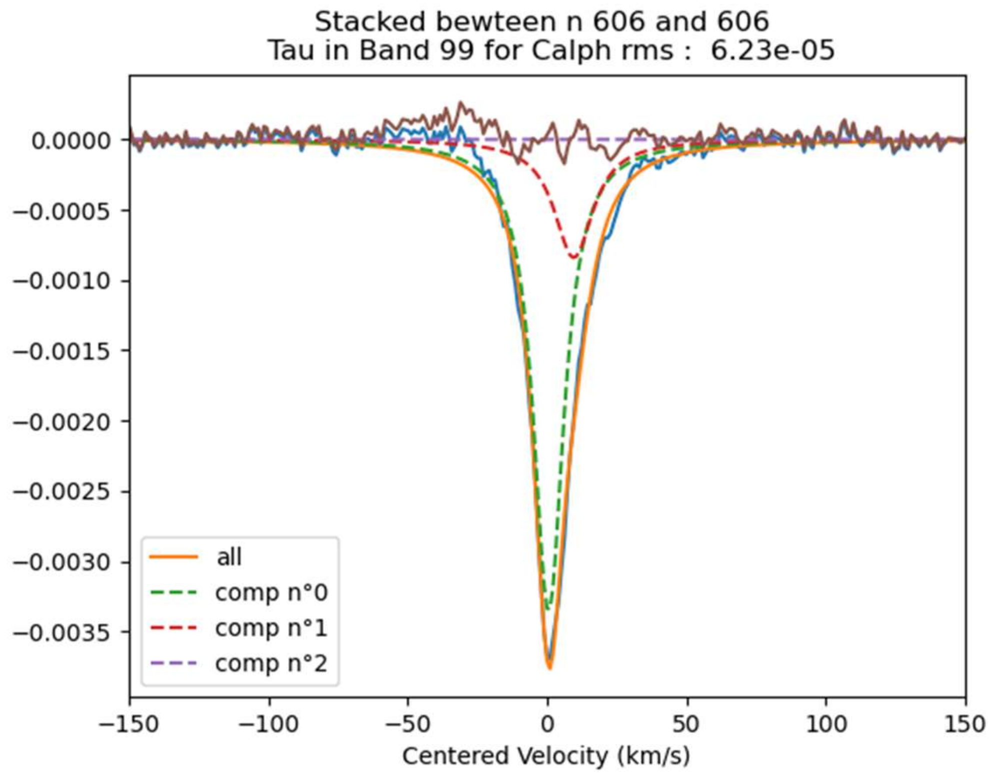

Results

Carbon RRLS in CAS A

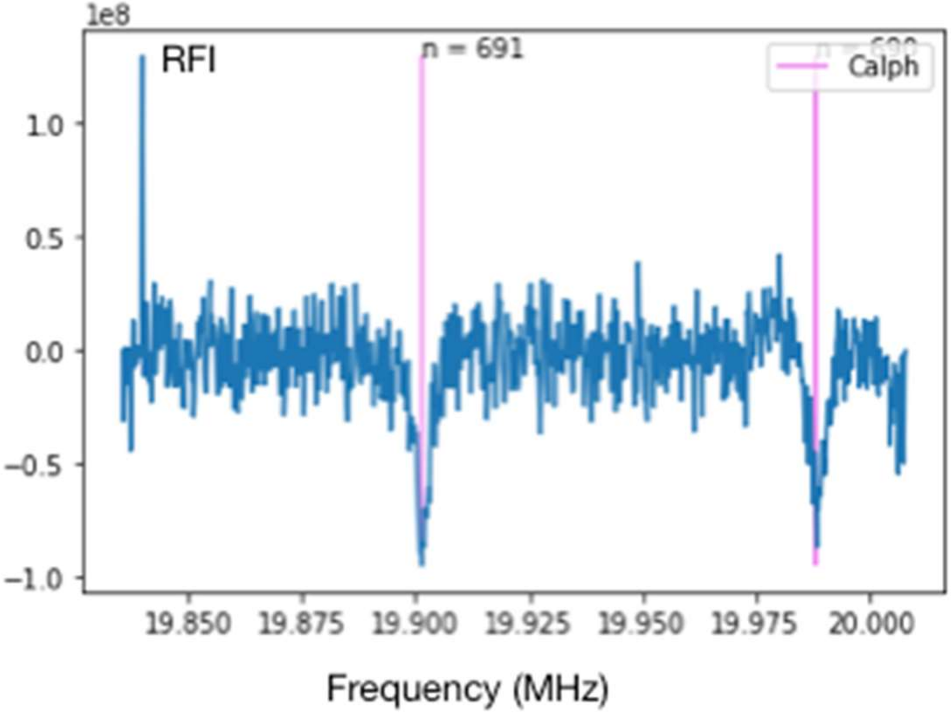

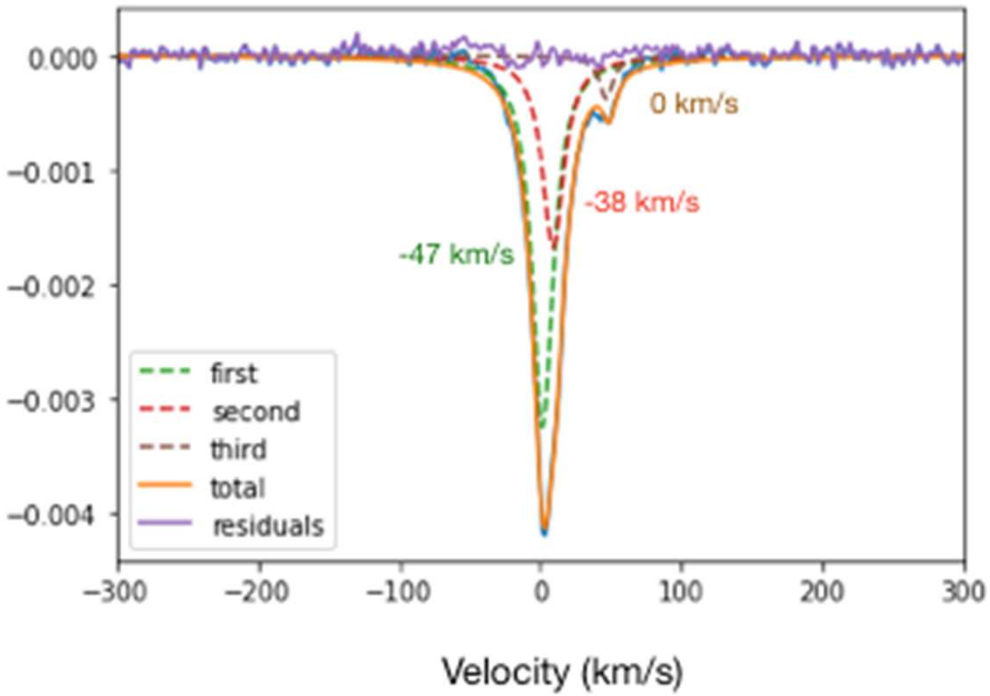

Carbon RRLS in Cas A

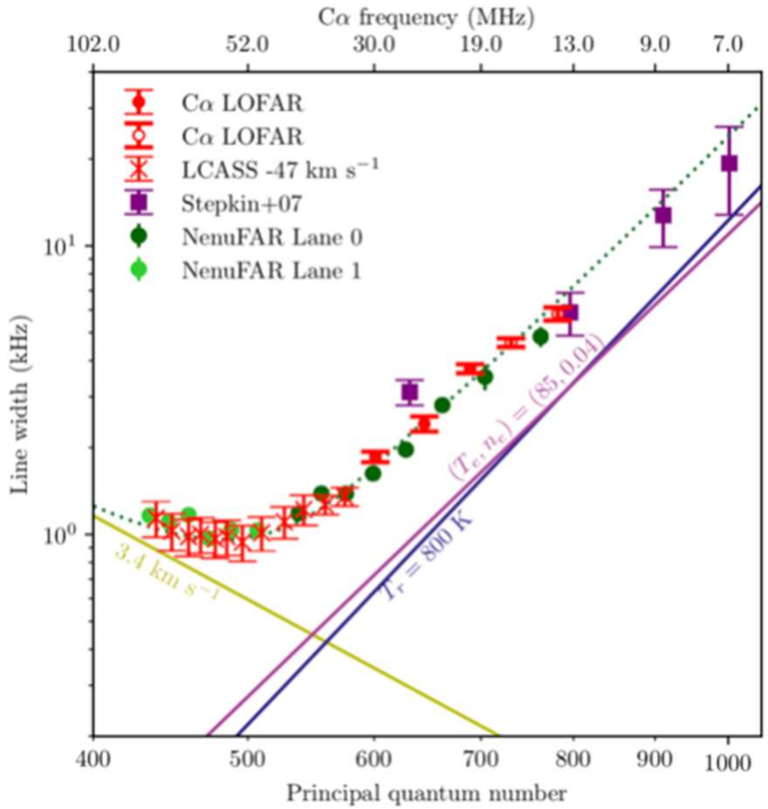

Fig. 3 Comparison of results obtained with NenuFAR and with LOFAR (Salas et al., 2017, Oonk et al., 2017). The measurement points represent the total widths of the Voigt profiles in kHz as a function of quantum number (average n of the stacked sample). The solid color curves represent

Python pipeline for RRLs

http://nenufar-rrl.obspm.fr/

…in progress

RRL

Search docs

CONTENTS:

rrl

» NenuFAR RRL Pipeline

View page source

NenuFAR RRL Pipeline

Radio-Recombination Line Pipeline

Introduction

This project documents the pipeline for data reduction of Radio Recombination Lines observed by NenuFAR in the Early-Science ES10 project. The main procedure is a pipeline that calls the L1 and calcul class fonction.

Outputs

The products are png files and pickles output.

- Python pickles
- PNG plots

Contents:

- rrl
  - L1_class module
  - Pipeline_stacking_fitting module
  - calcul module

RRL

Search docs

CONTENTS:

⊟ rrl

L1_class module

Pipeline_stacking_fitting module

calcul module

`calcul.a_Lorentz`*(area, gamma, sigma, fwhm)* [source]

area : integrated intensity (km/s) fwhm : full width half max of voigt (km/s) gamma : fwhm of lorentzian contrib. (km/s) sigma : fwhm of doppler contrib. (gaussian) (km/s)

`calcul.doppler_correction`*(f, v)* [source]

`calcul.doppler_corrections`*(mean_time, ra='23h23m24s', dec='58d48m54', obs_lat=47.367686, obs_lon=2.194313, obs_alt=150.0)* [source]

computes the projected velocity of the telescope wrt four coordinate systems: geo, helio, bary, lsr. To correct a velocity axis to the LSR do: vcorr = doppler_corrections(ra, dec, mean_time) rv = rv + vcorr[3] + rv * vcorr[3] / consts.c where rv is the observed radial velocity.

Parameters:
- **ra** – right ascension in degrees, J2000 frame.
- **dec** – declination in degrees, J2000 frame.
- **mean_time** – mean time of observation in isot format. Example "2017-01-15T01:59:58.99"
- **obs_lon** – East-longitude of observatory in degrees.
- **obs_lat** – Latitude of observatory in degrees.
- **obs_alt** – Altitude of the observatory in meters.

Returns: $Delta_v$ to add to the expected velocity

Return type: float

`calcul.extract_lines`*(HDU, quantum_nb, f_range, sub_range)* [source]

Entry : path_fits : str // path to the .spectra.fits data f_range : tuple // beginning and end of the frequency range where we look for lines sub_range : tuple // corresponding subband numbers Return : dict // containing sliced lines and corresponding : frequency and velocity ranges, rms value name of the dict : CASA + date

`calcul.f_to_v`*(f, f0)* [source]

First results on Cas A

…in progress

NenuFAR detects giant hydrogen and carbon atoms in the remnant of Supernova Cassiope A.

Recombination lines (including the iconic Hα in the optical domain) allow us to study the diffuse phases of the interstellar medium. In the Bohr formalism, the electrons of an excited atom are in discretized orbits; the diameter of an excited atom is then defined by d = n x 1.05 x 10-10 m (n being the main quantum level of excitation). In the diffuse interstellar medium where collisions are very rare, some atoms can be excited in extremely high quantum levels (n > 100), they are then called Rydberg atoms. These atoms have consequently classical diameters of the order of a few microns, the typical size of a bacteria or a fly ash on earth. When these giant atoms de-excite from such levels, they radiate their energy in the low frequency radio domain (< 1 GHz). These are the radio recombination lines (RRL). We have used NenuFAR, the large low frequency radio telescope (10 MHz to 85 MHz) of the Nançay station, precursor of SKA to observe these lines. We have detected them very easily in front of the synchrotron continuum emission source of the Cas A supernova remnant, confirming and complementing recent LOFAR results. The analysis of these new data, obtained in the framework of the Early Science Key Project ES10, (i) underlines the interest of RLLs (still little observed) for the study of the interstellar medium, (ii) confirms the potential of NenuFAR in this field and (iii) shows the possible perspectives in the context of SKA.

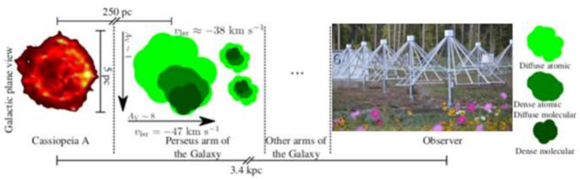

Fig. 1 Figure adapted from Salas et al, (2018). The supernova remnant Case A was observed by NenuFAR antennas in September 2019 in the 10-85 MHz frequency band. Data reduction and analysis was performed in spring 2021 by Lucie Cros. The results presented here correspond to a 2h sample of observations.

Observations

Obtained within the framework of the Early science ES10 project, the objective of these first observations was to determine precisely the capabilities of NenuFAR for the study of the Interstellar Medium via the observation of the recombination lines (RRL) in front of an emblematic source. We chose to point NenuFAR towards Cas A, whose continuum level is particularly high, which facilitates the detection of the lines in absorption. The results show that the instrument is up to its

…ith 2h of observation, NenuFAR reaches a signal-to-noise level of the order of …dividual lines and of the order of 7 times higher (SNR~20-70) when the stacking …n samples of 50 lines.

…method consists in stacking groups of lines to increase the signal-to-noise …he NenuFAR band allows to cover the expected absorption frequencies of a …bination lines (a hundred main de-excitation quantum level). Since all these …n the same absorber, it is possible to re-center and average them. This is a well …ue to increase the detection levels, by including the contribution to the signal of …-detectable lines.

…is required the implementation of a pipeline optimized for the detection of weak …h ~10-3) and narrow (a few km/s) absorption lines. A calibration of the spectral …ood accuracy was necessary to correctly estimate the continuum level over the … band and thus to determine the depths and line-widths of the different visible …. For this purpose, it was necessary to (i) remove the very large number of …FI) which pollute the low radio frequencies, (ii) correct the signal fluctuations with …all scales (in each of the 192 sub-bands of 195 kHz bandwidth each) and (iii) …olute flux as a function of frequency at large scales from the power spectrum of the …sion expected for Cas A, thus allowing an estimate of the noise level reached in …the predictions of the NenuFAR sensitivity estimator (https://github.com/AlanLoh/

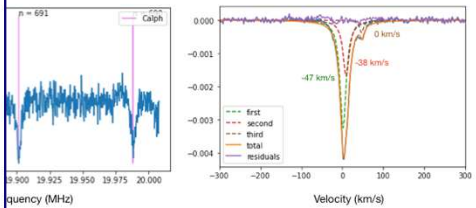

…eft: example of recombination lines of Carbon Cα at quantum level n=690 and …d and detected in absorption by NenuFAR. Right: after stacking and with a fit by …r each of the 3 components in velocity. The increase of the signal to noise ratio … different velocity structures in the line and thus to identify different components of …Medium located at different radial velocities. The spectral resolution is 191 Hz (~2 … can provide a spectral resolution down to 95 Hz.

Results : Absorption line profiles

…left shows two individual absorption lines at n=690 and n=691. It can be seen that …level has been removed; it is therefore a negative signal that we are trying to … right of this figure it is the stacked signal of several quantum levels around n=599 …d. We have also overlaid absorption models to account for the contribution of the … located along the line of sight. These well known clouds in the Perseus arm are at …km/s, -38 km/s and 0 km/s. What we seek to determine then, is the width of these … order to constrain the properties of the absorbing Interstellar Medium. | For … first component at -47 km/s it is necessary to determine precisely the broadening in …ently in Hz) of the green profile of Figure 2. This broadening depends of course on … of the other components.

… a valuable indicator

…line widths? The broadening of the recombination lines depends on three different …nisms: (i) a Doppler broadening related to the thermal agitation and turbulence of …) a radiative broadening, related to the interaction of the Carbon atoms with an …n field and (iii) a pressure broadening (also called collisional broadening), related to …with the electrons of the medium. If the Doppler broadening is well represented by … other mechanisms affect the wings of the line and require a Lorentzian profile. …ematical functions combined correspond to what is called a Voigt profile.

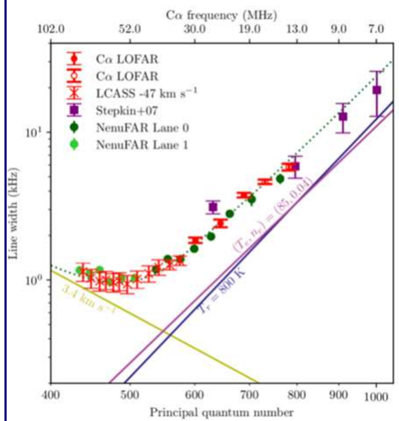

…on of results obtained with NenuFAR and with LOFAR (Salas et al., 2017, Oonk et … measurement points represent the total widths of the Voigt profiles in kHz as a function of quantum number (average n of the stacked sample). The solid color curves represent

…l model predictions for different local properties of the interstellar medium. The dashed …he sum of the three contributions.

…l quantum numbers (around 500), ie for smaller atoms, it is the Doppler broadening that …s and we expect the other contributions to be negligible. But when the atoms are larger …n=500), then it is the Lorentzian line wings that contribute to the bulk of the broadening. If …ure the line profiles for different quantum numbers, it is then possible to observe this … and to determine the properties of the interstellar medium (thermal and turbulent velocity … temperature of the external radiation; density and temperature of electrons at high n). This …ented in Figure 3, which also shows the agreement between the NenuFAR data and those … with LOFAR over the whole low frequency range covered.

…ces

…t al., in prep.
…M. A. et Sorochenko, R. L., 1992, SSRv, 59, 412G
…et al. 2017, MNRAS, 465, 1066O
…t al., 2018, MNRAS, 475, 2496S
…t al., 2017, MNRAS, 467; 2274S
…F. et al., 2017, ApJ, 837; 142

… Contacts

…os
… ENS, PSL, France

…Gusdorf
…e Recherche CNRS, ENS, PSL, France

…Salomé
…ne-Adjoint, Observatoire de Paris, PSL, France

…dro
…ank Observatory, 155 Observatory Road, Green Bank, WV 24915, USA

Perspectives

Other low radio sources

Source name	Coordinates		Flux density (Jy)			Size[a]
	RA (J2000)	DEC (J2000)	@ 50 MHz	@ 150 MHz	@ 1.4 GHz	(arcmin)
Cassiopeia A (3C 461)	$23^h23^m27.94^s$	$+58°48'42.4''$	27104	9856	1768	7.4
Cygnus A (3C 405)	$19^h59^m28.35^s$	$+40°44'02.1''$	22146	10713	1579	2.3
Taurus A (3C 144, M 1, Crab Nebula)	$05^h34^m31.97^s$	$+22°00'52.1''$	2008	1368	829	7.9

- Confront the reduction pipeline to lower and lower flux density
  1. Cassiopeia A
  2. Cygnus A
  3. Taurus A

Cygnus A with LOFAR

Stack	Range (MHz)	Range (n)	Centre (km s^{-1})	FWHM (km s^{-1})	$\int \tau \, dv$ (km s^{-1})	τ_{peak}
ALL	33–57	487–583	3.8 ± 1	10.0 ± 3	$(2.1 \pm 0.4) \times 10^{-3}$	$(2.2 \pm 0.5) \times 10^{-4}$
LOW	33–43	535–583	2.9 ± 1	19.0 ± 5	$(3.3 \pm 0.8) \times 10^{-3}$	$(1.8 \pm 0.6) \times 10^{-4}$
MID	39–49	512–552	2.8 ± 1	9.8 ± 3	$(2.1 \pm 0.6) \times 10^{-3}$	$(1.9 \pm 0.6) \times 10^{-4}$
HIGH	44–57	487–530	4.5 ± 1	5.8 ± 2	$(1.6 \pm 0.5) \times 10^{-3}$	$(2.6 \pm 0.7) \times 10^{-4}$

10x lower than Cas A

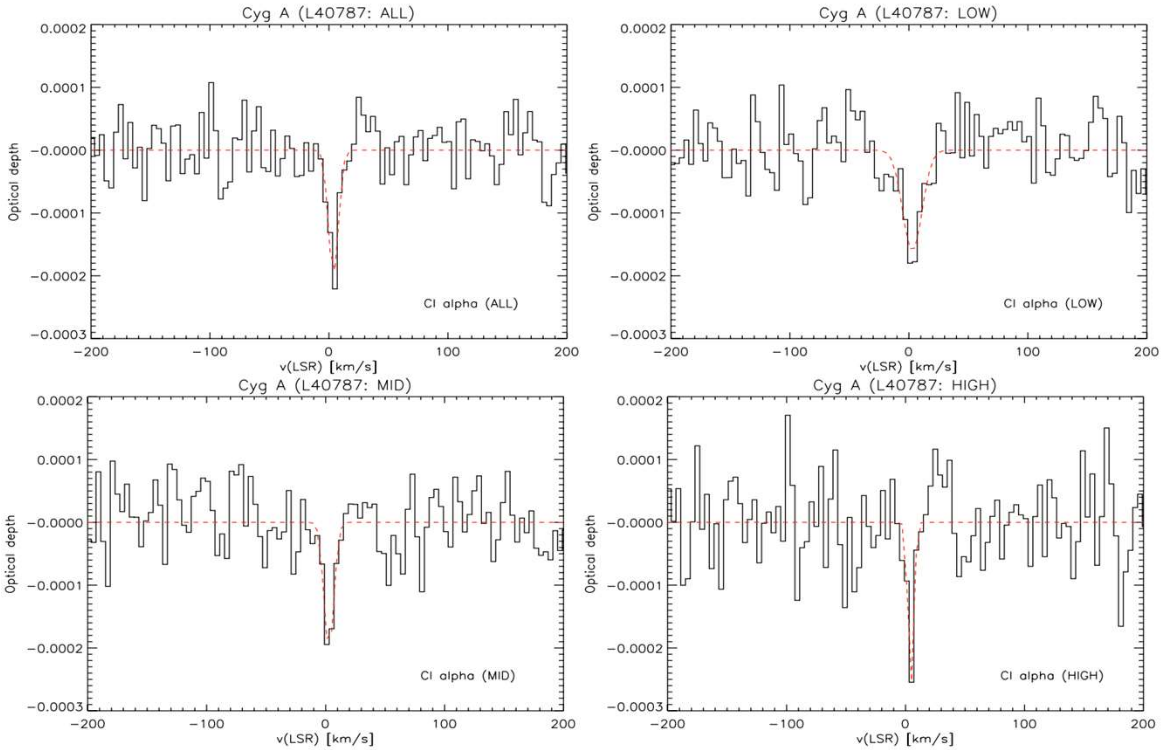

Cygnus A with NenuFAR

Parameter	Value	
Source	Cyg A	
Field centre RA (J2000)	19 :59 :28.3	
Field centre Dec. (J2000)	40 :44 :02	
Observing date	2021 October 19	16h-18h
Observing date	2021 October 19	18h-22h
Observing date	2021 October 20	16h-17h30
Observing date	2021 October 20	17h30-19h30
Observing date	2021 October 20	19h30-21h30
Observing date	2021 October 21	21h-22h
Observing date	2021 October 21	22h30-23h30
Observing date	2021 October 22	20h-22h
Observing date	2021 October 22	22h-00h

Parameter	Value
Frequency range	10-85 MHz
Number of subbands	2×192
Width of subband	0.1953 MHz
Channels per subband	1024
Velocity resolution	0.7-5.7 km/s

- Data reduced
- Analysis on-going

+ 40 hours on source to be available soon

Taurus A

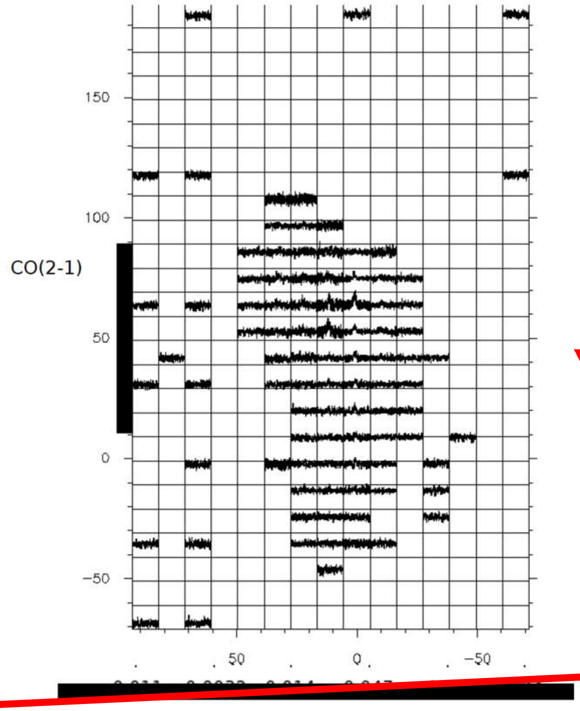

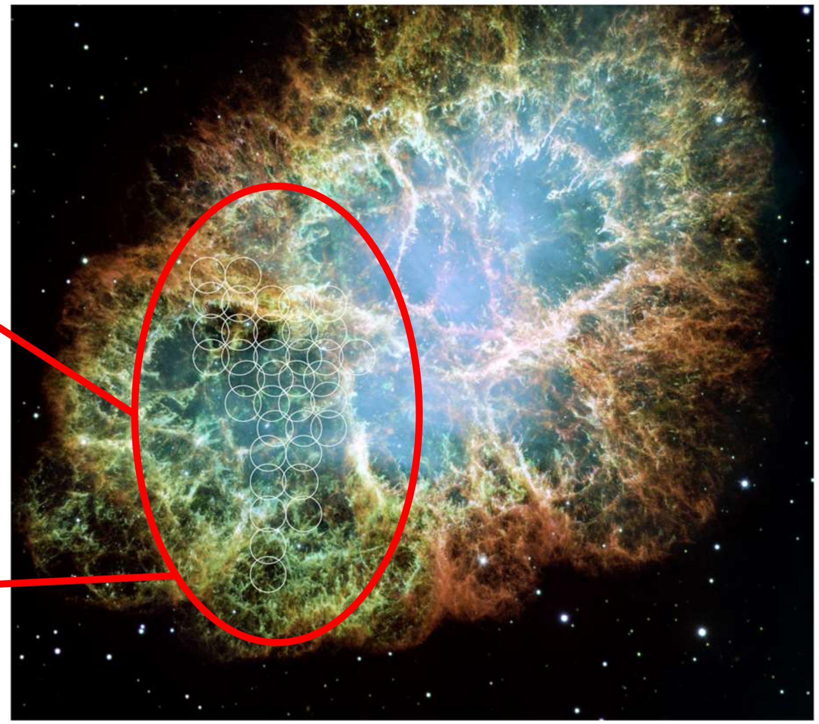

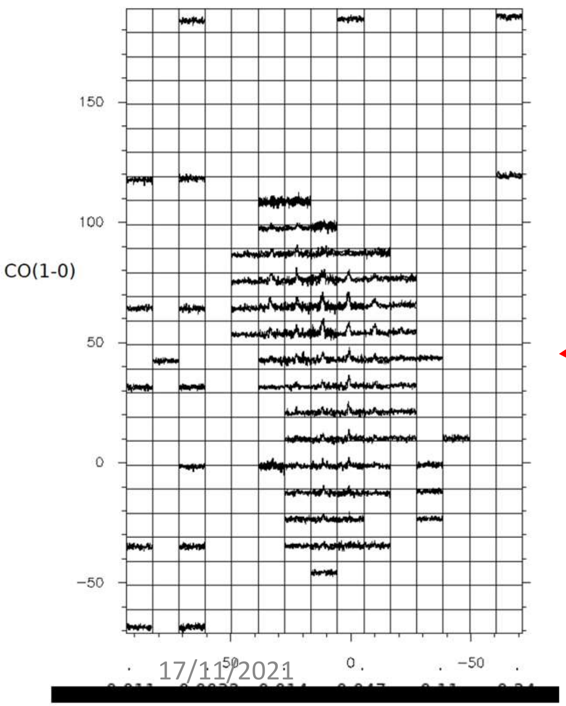

Coupling LOFAR and NenuFAR : some great expectations

- Better spatial resolution => cartography of hot clouds in ISM

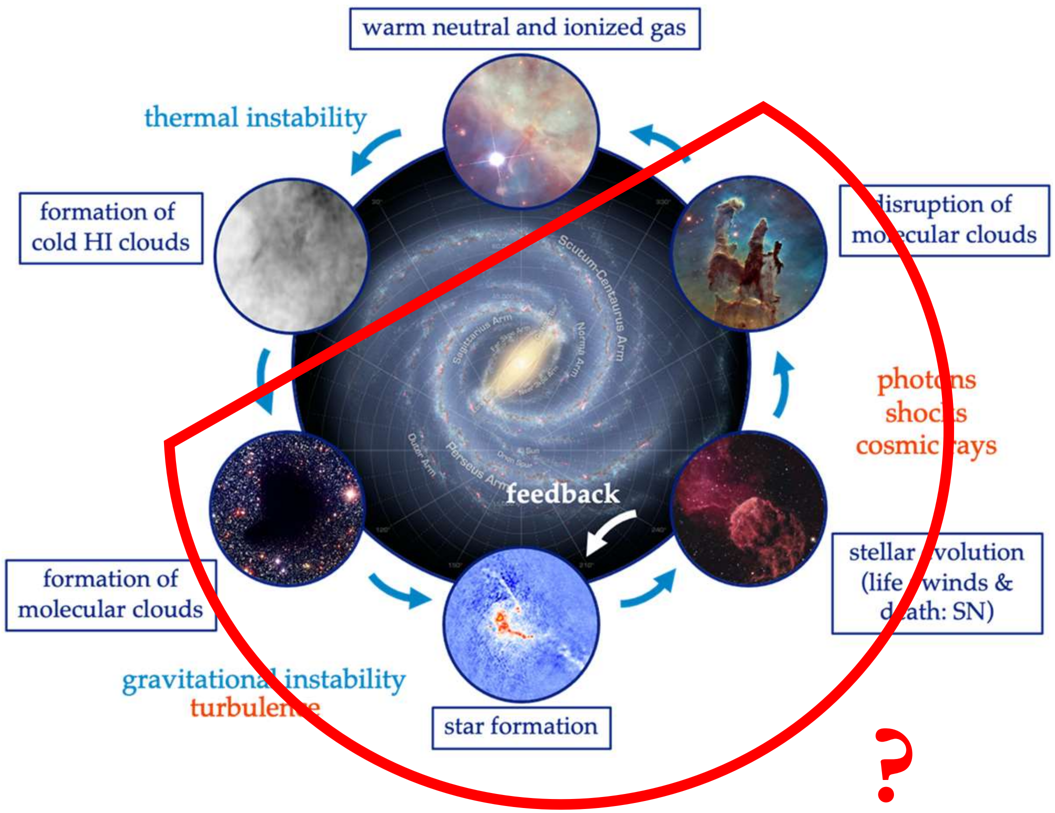

- Opens the way to RRL detections in the other stages of the ISM cycle !

From all the ES10 team, thank you !